THE UNIVERSITY OF READING

Department of Mathematics

Investigation of waiting times in non-linear diffusion equations using a moving mesh method.

Jovan D. Stojsavljevic

August 2007

This dissertation is submitted to the Department of Mathematics in partial fulfilment of the requirement for the Master of Science.

Abstract

In this study we look at the waiting time phenomenon with regards to the porous-medium equation and the thin-film equation. The study begins by deriving an equation for the velocity using a conservation of mass principle, and is used to analyse which initial data exhibit zero velocity at the boundaries at $t = 0$. An advection-diffusion equation for the velocity is then derived to examine the behaviour of velocity during the waiting time period. This is numerically solved using a simple mixed upwind finite difference scheme. A moving mesh finite element method is then derived for the porous-medium and thin film equations and an in depth discussion follows on the numerical solutions. Finally the work is extended by studying the Richards' equation and applying the analytical methods used in the dissertation and the moving finite element method to it. The results are then discussed.

I confirm that this is my own work, and the use of all material from other sources has been properly and fully acknowledged.

Acknowledgements

This dissertation would not have been possible without the supervision of Mike Baines, whose support, enthusiasm and never ending patience have been invaluable. My thanks extend to other members of staff and fellow postgrads in the maths department.

I owe special thanks to Amaryllis Paidousi for the endless love, encouragement and support she provided during the time spent on this dissertation as well as my parents who have constantly believed in me, without them I do not think I would be writing this.

Finally the financial support provided by the National Environment Research Council during this MSc has been very important in the completion of this study.

Contents

List of Figures

Chapter 1

Introduction

Partial differential equations (PDEs) are frequently used to describe physical phenomena such as the propagation of sound or heat, fluid flow and physical laws such as the conservation of mass, energy or momentum. Their solutions provide an insight to the physical process they are modelling, by providing information on some quantity throughout a domain. The domains can be fixed, but more interestingly they can be dictated by their solution. These types of problems are usually classified as moving or free boundary problems and are ubiquitous in the mathematical description of physical processes.

Moving boundary problems have had little attention until recently, when in the 1960s, due to their relevance in diffusion and heat flow processes, a modern approach to the theory of non-linear PDEs brought new insight and methods to investigate this phenomenon.

During this interest in moving boundary problems, a phenomenon was discovered with regards to the time dependent PDEs, where the boundary would initially wait for a period of time before it moved. This phenomenon is called the waiting time and has been found to occur in several different equations including the shallow water equation and the non-linear diffusion equations.

This dissertation will investigate the waiting time phenomenon of the evolutionary, degenerate, second and fourth order non-linear diffusion equations by using a moving mesh finite element method [3].

We begin with a look at the applications of nonlinear diffusion. Both the porous-medium equation (PME) and the thin-film equation (TFE) will be presented in detail with a brief mention of the Richard's equation.

In Chapter 3 we focus on the waiting time phenomenon and discuss the existing literature. The results and methods presented in these papers will be used for both analytical and numerical purposes throughout the dissertation.

Then, in Chapter 4, a conservation of mass law will be used in conjunction with both the PME and the TFE to derive the velocity of u across the whole region and importantly, with regards to waiting times, the velocities at the boundaries of the domain.

The initial conditions play a very important role in whether the waiting time phenomenon will occur, so in Chapter 5, using the velocity derived in the previous chapter, the intitial behaviour of the boundary will be investigated. This analysis gives particular cases for when the waiting time will occur, but gives no clues as to the duration of the waiting time, or to the behaviour of the boundaries for $t > 0$.

In Chapter 6, we examine the velocities for $t > 0$ by constructing an advection-diffusion equation for the velocity in terms of v and u. We shall use the results that the method of characteristics give and explain why they are unsuitable for this problem, followed by a derivation of a numerical approximation and then finally a discussion of the results.

Then in Chapter 7, we shall derive the moving finite element method that will be used to numerically solve both the PME and the TFE. Near the end of the chapter, a discussion of the methods used to computationally solve these equations will be offered.

In Chapter 8, we present the numerical results obtained by using the moving finite element method and explain them in detail, noting in particular the shock formations and front movements that occur.

In the penultimate chapter, we shall focus our investigations on the Richards' equation. This involves the use of the analytical and numerical methods described in the previous chapters. The numerical results shall be briefly examined.

Finally a summary of the dissertation will be presented, including the results from our investigations. Then we end on a discussion of possible further work.

Chapter 2

Non-Linear Diffusion

This dissertation is primarily concerned with one-dimensional non-linear diffusion equations of the form

$$u_t = (-1)^n \left(D(u) \frac{\partial^{2n+1} u}{\partial x^{2n+1}} \right)_x \tag{2.1}$$

It describes physical situations such as the heat conduction in a one-dimensional solid body, insect population dispersion and the spread of liquid on a surface. In particular, problems in which the diffusion coefficient takes the form $D(u) = u^n$, where $n > 0$ is a diffusion growth exponent, will be investigated.

Equation (2.1) is derived from the generalised Reynolds equation

$$u_t = (u^n p_x)_x \tag{2.2}$$

with p being a pressure which determines the order of the equation. For example, for the thin-film equation, we have

$$p = -\frac{\partial^2 u}{\partial x^2}$$

Here, p represents a pressure due to surface tension, for example, when modelling the capillary effects of a thin liquid film on a solid surface.

In this chapter we shall look at some applications of (2.2) in an attempt to motivate interest in the generation of numerical solutions that exhibit the waiting time phenomenon and also briefly examine the literature currently available.

2.1 The Porous-Medium Equation

The PME is of the form

$$u_t = \left(u^n u_x\right)_x \tag{2.3}$$

where n is as stated above and with $u = 0$ at the boundary.

There are many different applications by varying n that naturally arise in the study of physical problems. When $n = 1$, the equation models the flow in thin saturated regions in a homogeneous isotropic porous media [14]. This equation is also known as the Boussinesq equation when an impermeable boundary is set at $x = 0$.

When $n \geq 1$, it provides a model for the percolation of a compressible gas through porous media, neglecting gravity [19]. With $n = 3$, the equation (2.3) models thin viscous liquid films spreading under gravity over a horizontal plane [17].

In Chapter 9, we extend the second order differential equation by adding an extra term. This equation is the nondimensionalised Richards' equation and is of the form

$$s_t = \left(s^{k-2} u_z + s^k\right)_z$$

where $s = s(z, t)$ is the saturation of the wetting phase at height z.

This equation models the distribution of a wetting fluid within an artificially saturated porous medium, subject to capillary pressure and gravity, [9], [23]. When $k = 3$, this equation models the flow of a dense non-aqueous

phase liquids (DNAPLs). The equation is used to estimate the time that the pollutant takes to reach the water table. This is an increasingly important application due to the danger that soil contaminated with DNAPLs poses to the environment.

The study of the waiting time phenomenon with regards to this problem is an important and interesting extension to the literature that is currently available. If the profile of the saturation of the liquid has to rearrange itself before the boundary moves, this will affect estimates on how long the pollutant will stay at a certain depth until it starts seeping deeper into the soil.

As can be seen, the second order case (2.3), is very important due to its broad range of applications, and has hence been studied extensively using different analytical and numerical methods. Similarity solutions have been found [4], as well as solutions that illustrate the behaviour of the waiting time phenomenon [15] and solutions that have been constructed using singular perturbation theory [12]. Numerical approximations include finite difference moving mesh methods [5], fixed grid methods with multi-grid solvers and the method that will be used throughout this thesis, namely the adaptive mesh finite element method used for solving time-dependent PDEs. [2], [3].

2.2 The Thin-Film Equation

The TFE is of the form

$$u_t = -\left(u^n u_{xxx}\right)_x$$

where again, n is as stated previously, and with $u = 0$ at the boundaries being considered.

With the diffusion growth exponent $n = 3$, the equation models the lubrication of a surface tension driven thin viscous liquid spreading on a horizontal

surface with a no-slip condition at the solid/liquid/air interface, [4], [20].

The no-slip condition implies that an infinite force occurs at the interface, but this is avoided when $0 < n < 3$, and instead we have a Navier-type slip condition. Mathematically this is shown by the fact that self similar source-type solutions only exist if $n < 3$ [6]. These values of n apply to problems concerned with the spreading or non-spreading of liquids. Another application is the runoff of rainwater over soils and the spreading of fluid on textiles. Momoniat and Mason addressed this in their paper [18] and called it the spreading of a thin film with suction or blowing.

Again, there is a lot of literature with regards to the TFE, and as with the PME, it has been solved using similar analytical and numerical methods. Most importantly, using asymptotic methods and a multi-grid solver, Blowey et al [6] [16] have some important results that will be used as a comparison in chapters 5 and 9.

Continuing with the literature review, the next chapter shall focus on the waiting time phenomenon by looking at the physical applications and the recent developments in the field.

Chapter 3

Existence of Waiting Times

The waiting time phenomenon can be defined as being the finite non-zero time for which the free boundary is stationary. Typically, during this time, the initial density profile redistributes itself before the boundary begins to move.

This phenomenon was initially conjectured by Knerr [13] for the PME, and then was further investigated by Lacey et al [15]. They noted two applications for the waiting time solutions of the PME. It had been observed that regions of water vapour in dry powder remained localised for periods of time before spreading out. The second application was discovered after observations of a blob of viscous liquid placed at rest on a horizontal surface had a stationary perimeter for a non-zero time interval before spreading out under gravity. It is worth noting that the observer commented on the fact that this stationary perimeter only occurred during certain initial profiles of the liquid blob. Lacey et al. found that this was shown mathematically with the self similar solution they constructed, and in Chapter 5, we shall see that this plays an important role in selecting initial conditions for which the waiting time phenomenon occurs.

The rest of the chapter will look at the important analytical and numerical

results from the literature available for the PME and the TFE.

3.1 Waiting Times of the Porous Medium Equation

As mentioned previously, Knerr [13] proved the existence of waiting time solutions. His work, (along with Aronson and Kamin) spurred on further investigations which shall now be discussed in further detail as they contain important results.

Lacey and Ockendon [15] initially looked at the waiting time solutions of the PME by constructing similarity solutions that, when prescribed with appropriate initial data, demonstrated a boundary that exhibited waiting time behaviour and also continued to exist after the interface began to move. Using a comparison theorem developed by Oleinik et al [21], they found lower and upper bounds on the waiting time that significantly improved on results found by Aronson et al [1]. They concluded that the dependence of waiting times upon the global properties of the intitial data $u_0(x)$ was clear. Later on in this dissertation, after deriving the velocity using a conservation of mass argument in Chapter 4, we can analyse initial data to see whether the initial velocity at the boundary is zero, implying a waiting time.

The next major development in the literature on this subject was Kath and Cohens paper [12]. Their motivation was to improve on earlier works by using a different method to approximate bounds for the waiting time. They used singular perturbation theory in the limit of small n which allowed them to construct solutions for initial conditions that were not solvable by similarity methods.

Kath and Cohen discussed 'corner shocks' which were used to indicate a discontinuous jump in the first derivative of u wrt x. Coincidentally, when

using the conservation of mass principle in Chapter 4, we arrive to a velocity for the movement of the fluid $v = -u^{n-1}u_x$. In Chapter 8 we shall investigate numerical solutions where $n = 1$ and show that as the velocity changes with time, if the waiting time behaviour is to occur, a shock appears at the interface in the velocity just before the boundary begins to move, ending the waiting time period. See, figure (8.3).

Kath and Cohen also mention corner layers which are when u_x changes significantly within Δx. This is a direct result which has also been observed in the numerical solutions computed in this dissertation. See figure (8.2).

The work of Gratton and Vigo [8] uses a power law type initial condition, $u \propto x^p$. Using asymptotic methods, they found that by fixing $n = 3$ (from the already defined PME equation (2.3)), the boundary exhibited different behaviour for different values of p. This work is extended in Chapter 5 for $n > 0$.

Gratton and Vigo numerically solved the PME using a three-level second order implicit finite difference scheme, centred in both time and space. Their numerical investigations gave "... results in harmony with [the] theory".

3.2 Waiting times of the Thin-Film Equation

The TFE has not been studied in as much detail as the PME but recently there has been more interest in the behaviour of similarity solutions. Despite this, there have been asymptotic solutions for small n [25](similar to Kath and Cohens work on the PME), small time conjectures [16], constructing simple waiting time solutions [25] and numerical solutions [6].

Smyth and Hill [25] comment on how in some respects the properties and solutions of the TFE are similar to those of the PME. Using an asymptotic solution of the TFE, they find that in contrast to the solutions for the PME,

when $0 < n << 1$, the solutions tended to have an infinite waiting time, yet the solutions were not valid for large times.

As mentioned previously, Blowey, King and Langdons paper examines small and waiting time behaviour for $0 < n \leq 4$. Their formal asymptotic results will be compared with the results found in Chapter 5. The numerical results that they found were computed on a fixed grid with a multi grid solver and they will be used as a comparison to the results we get for the TFE.

After reviewing the literature, we shall now move on and derive an equation for the velocity using a conservation of mass law. For both the analysis and the numerical method, this is a fundamental part of the dissertation.

Chapter 4

Conservation of mass

In this chapter we shall derive the velocity of the boundary by using a conservation of mass principle. This states that the mass of a quantity in a closed system will remain constant, regardless of the processes acting inside the system.

The boundary velocity of the generalised Reynolds equation will be derived with the initial condition $u = u_0$.

We begin by integrating (2.1) w.r.t. x over the whole region and then applying the Reynolds transport theorem [26] to get an equation of the form

$$\begin{aligned} \frac{d}{dt}\int_{a(t)}^{b(t)} u dx &= \int_{a(t)}^{b(t)} \left(\frac{\partial u}{\partial t} + \frac{\partial}{\partial x}(uv)\right) dx \\ &= \int_{a(t)}^{b(t)} \frac{\partial u}{\partial t} dx + [uv]_{x_0}^{x_N} \end{aligned}$$

where $a(t)$ and $b(t)$ are the boundaries. Substituting in equation (2.2), leads to

$$\begin{aligned}\frac{d}{dt}\int_{a(t)}^{b(t)} u dx &= \int_{a(t)}^{b(t)} \left(u^n p_x\right)_x dx + \left[uv\right]_{a(t)}^{b(t)} \\ &= \left[u^n p_x + uv\right]_{a(t)}^{b(t)}\end{aligned}$$

Applying the boundary conditions $u = 0$ at $a(t)$ and $b(t)$, we arrive to the conservation of mass over the entire region $\forall t$.

$$\begin{aligned}\frac{d}{dt}\int_{a(t)}^{b(t)} u dx &= \left[u^n p_x + uv\right]_{x_0}^{x_N} = 0 \\ &\Longleftrightarrow \\ \int_{a(t)}^{b(t)} u dx &= constant\end{aligned}$$

To be able to calculate the interior velocities, we shall now consistently define a local conservation of mass principle for any interval $(x_{i-1}(t), x_i(t))$

$$\int_{x_{i-1}(t)}^{x_i(t)} u dx = constant \tag{4.1}$$

Applying Liebniz' Integral rule to (4.1) $\forall t$, yields

$$\frac{d}{dt}\int_{x_{i-1}(t)}^{x_i(t)} u dx = \int_{x_{i-1}(t)}^{x_i(t)} \frac{\partial u}{\partial t} dx + u(x_i(t), t)\frac{\partial x_i}{\partial t} - u(x_{i-1}(t), t)\frac{\partial x_{i-1}}{\partial t} \tag{4.2}$$

giving

$$\left[u^n p_x + vu\right]_{x_{i-1}(t)}^{x_i(t)} = 0$$

By setting $x_{i-1}(t) = a(t)$ leads to

$$u^n p_x + vu = 0 \tag{4.3}$$

for all $x = x_i(t)$ Rearranging (4.3), we get

$$v = -u^{n-1}p_x \tag{4.4}$$

To find the velocity at the boundaries, we must take

$$v = -\lim_{u \to 0} u^{n-1}p_x \tag{4.5}$$

An equation for the velocity of the fluid has been derived by conserving mass within the domain. This can be used to find out the behaviour of the boundary at $t = 0$, which we shall investigate in the next chapter. We shall also later on, construct an equation in terms of v and its derivatives (see Chapter 6). This will enable the investigation of the behaviour of the velocity during the waiting time. To see the behaviour of the velocity during and after the waiting time, a moving finite element method using (4.4) will be constructed in Chapter 7.

Chapter 5

Initial Behaviour of the boundary

In this chapter we shall look at the intitial behaviour at the boundaries by using the velocity equation derived in the previous chapter. The initial conditions we shall use for the numerical solutions of the PME and the TFE were chosen so as to be comparable with previous numerical solutions by Blowey et al. [6].

This has been investigated briefly for the PME, but in a lot more detail for the TFE by Langdon [16], and Blowey et al. [6] for initial conditions of the general form

$$u(x,0) = A_0 \left(x_B - x^2\right)^\alpha$$

As mentioned we shall use the initial data already studied. This is of the form

$$u(x,0) = 5\left(\frac{9}{16} - x^2\right)^\alpha \tag{5.1}$$

For the initial data to remain positive, we shall require the initial domain to be $x \in [-0.75, 0.75]$.

This initial data, combined with equation (4.5), can provide information about the velocity of the fluid at the boundary at $t = 0$. The two equations will be looked at in turn.

5.1 Analysis of the Initial data for the Porous-Medium Equation

We start by differentiating the initial data and substituting it into equation (4.5), we have

$$\begin{aligned} v_B &= -\lim_{u\to 0} u^{n-1}u_x \\ &= (5)^{n-1}10\alpha \lim_{x\to\frac{3}{4}} x\left(\frac{9}{16}-x^2\right)^{n\alpha-1} \end{aligned}$$

From this it is clear that there are three cases involved. They are

- If $n\alpha < 1$, $v_B \to +\infty$ as $x \to \frac{3}{4}$.
- If $n\alpha = 1$, then $v_B = (5)^{n-1}\frac{30}{4}\alpha$, finite and positive.
- If $n\alpha > 1$, $v_B = 0$.

We shall investigate when $n\alpha > 1$ as this shows that there is a waiting time before the boundary begins to moves. Figure (5.2) shows the initial velocities between 0.5 and the boundary 0.75.

5.2 Analysis of the Initial data for the Thin-Film Equation

For the TFE, as expected, we see a more varied behaviour. Letting $p = -u_{xx}$ and substituting from the third derivative of the initial data (5.1), we get

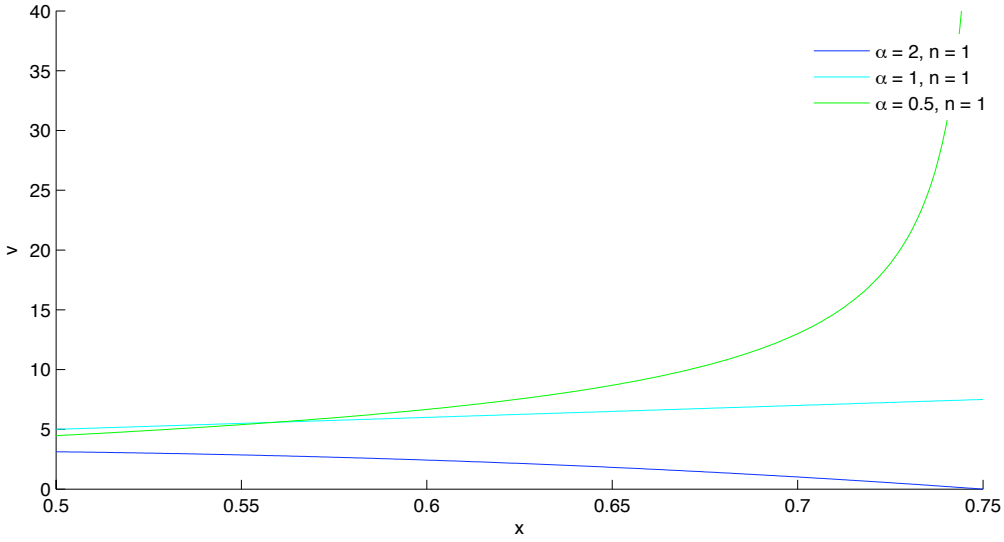

Figure 5.1: *Initial velocities of the PME using the intitial condions (5.1)*

$$\begin{aligned} v_B &= \lim_{u\to 0} u^{n-1}u_{xxx} = (5)^{n-1}60\alpha(\alpha-1)\lim_{x\to\frac{3}{4}} x\left(\frac{9}{16}-x^2\right)^{n\alpha-2} \\ &\quad -(5)^{n-1}40\alpha(\alpha-1)(\alpha-2)\lim_{x\to\frac{3}{4}} x\left(\frac{9}{16}-x^2\right)^{n\alpha-3} \end{aligned}$$

The special case of $\alpha = 2$, gives

$$v_B = (5)^{n-1}120\lim_{x\to\frac{3}{4}} x\left(\frac{9}{16}-x^2\right)^{2n-2}$$

we have the following behaviour

- if $n > 1$ $v_B = 0$.
- if $n = 1$ $v_B = 90$.
- if $n < 1$ $v_B \to +\infty$.

Also, another special case is if $\alpha = 1$, then $v_B = 0$.

Suppose that $\alpha \neq 2$ or 1. Then

- If $n\alpha > 3$, $v_B = 0$.
- If $n\alpha = 3$, $v_B = -(5)^{n-1}30\alpha(\alpha-1)(\alpha-2)$ and is therefore finite, positive or negative, depending on n and α.
- If $n\alpha < 3$, $v_B \to \pm\infty$ as $x \to \frac{3}{4}$,

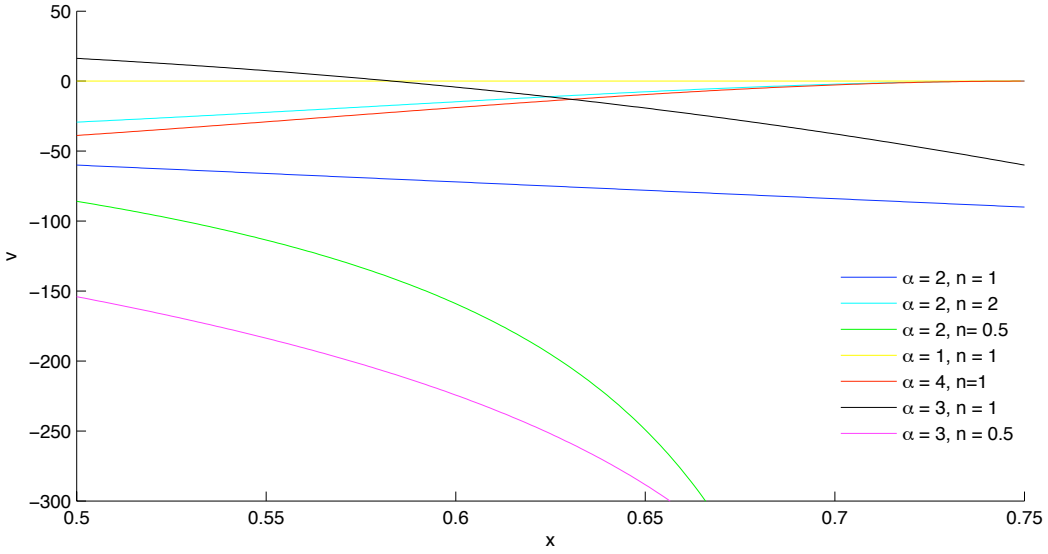

Figure 5.2: *Initial velocities of the TFE using the intitial condions (5.1)*

These results for the PME and the TFE coincide with Blowey, King and Langdons results [16].

The analysis of the velocity equation at the boundary has resulted in certain initial data having a waiting time period. In the next chapter an advection-diffusion equation will be constructed to see the behaviour of the velocity during the waiting time and we shall implement the results found in this chapter.

Chapter 6

Velocity advection-diffusion equation

Using equation (4.4), an advection-diffusion equation in terms of v can be derived to investigate the behaviour of the velocity during the waiting period.

6.1 The velocity equation for the PME

By differentiating equation (4.4) w.r.t. t and substituting in the PDE of the form $u_t = -(uv)_x$, we arrive to

$$v_t + (2+n)vv_x = u^n v_{xx} \tag{6.1}$$

As can be seen, u is still part of the equation. This is unavoidable, and hence to get a numerical solution we must solve for u also.

First off, it is simpler to deal with equation (6.1) by time splitting it into two equations

$$v_t + (2+n)vv_x = 0 \tag{6.2}$$

$$v_t = u^m v_{xx} \tag{6.3}$$

Clearly equation (6.2) is an advection equation, and (6.3) is a second order diffusion equation.

We shall use the method of characteristics to solve the advection part of the PDE by finding curves in the $x-t$ plane that reduce the equation to an ordinary differential equation (ODE). We shall look at the curves given by $\frac{dx}{dt} = a(u) = a(u_0)$ with the condition that $\frac{du}{dt} = 0$.

Using the method of characteristics, the characteristic solution of equation (6.2) is $v = v(x_0)$ on the line $x = (2+n)v(x_0)t + x_0$, allowing crossing and shock formation. This is evident as we are dealing with non-linear terms in (6.2). However, the effect of (6.3) is to smooth the shock. By using the results we had from analysing the initial data in the previous chapter, if we set $n\alpha > 1$, then we know that analytically, the velocity at the boundary $v_B = 0$, and hence the boundary waits.

Further quantitative analysis of this isn't useful as it is very difficult to implement the second equation (6.3). This acts as a damper or diffuser and prevents any useful results using characteristic analysis on the advection equation.

These analytical results on equation (6.2) coincide with Cath and Cohens [12] analysis of the corner shocks which occur at the time the boundary begins to move after an initial waiting time.

To solve (6.1) numerically it helps to first transform (6.1) into the form

$$v_t + \frac{2+n}{2}(v_x)^2 = u^n v_{xx}$$

Now we can solve this using a standard upwind finite difference method for the first derivatives w.r.t. t and x, and due to the damping effect of the u^n term, we can simply take a central difference method for the second derivative of v.

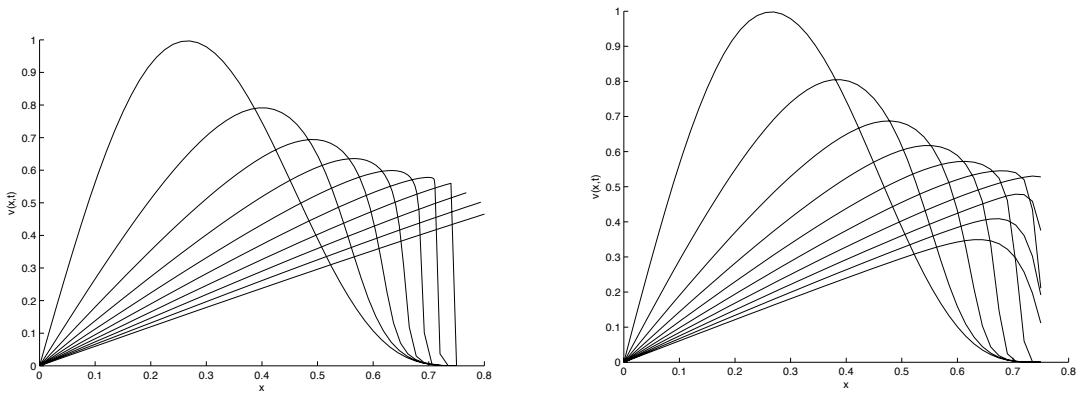

Figure 6.1: *Figure on the left shows the velocity that the moving mesh method calculates (see Chapter 7) and the figure on the right shows the numerical solution of equation (6.1).* $\alpha = 4.5$, $n = 1$.

$$\frac{v_j^{k+1} - v_j^k}{\Delta t} = (u_j^k)^n \left(\frac{v_{j+1}^k - 2v_j^k + v_{j-1}^k}{(\Delta x)^2} \right) - \frac{2+n}{2} \left(\frac{\left(v_j^k\right)^2 - \left(v_{j-1}^k\right)}{\Delta x} \right)$$

where k is the time step $t = k\Delta t$ and j is the spacial step $x = j\Delta x$.

Since we are solving for u on a moving mesh (see chapter 7), we must interpolate the solution to the points close by. Fortunately u is smooth when u is not small, so this can be calculated using a simple linear interpolation technique.

The numerical solution shows some interesting results (fig. (6.1)). The shock is formed and begins to move at a finite speed at approximately the same time as the boundary starts to move when solving the PME using a moving finite element method in Chapter 7.

It can be seen in figure (6.2) that the numerical solution of the advection-diffusion equation begins to move before the shock breaks in the mesh velocity plot. This shows the errors between the moving mesh method when solving the PME and the finite difference method used for the advection-diffusion equation. Analytically, we saw that for the PME, when $n\alpha > 1$, a waiting

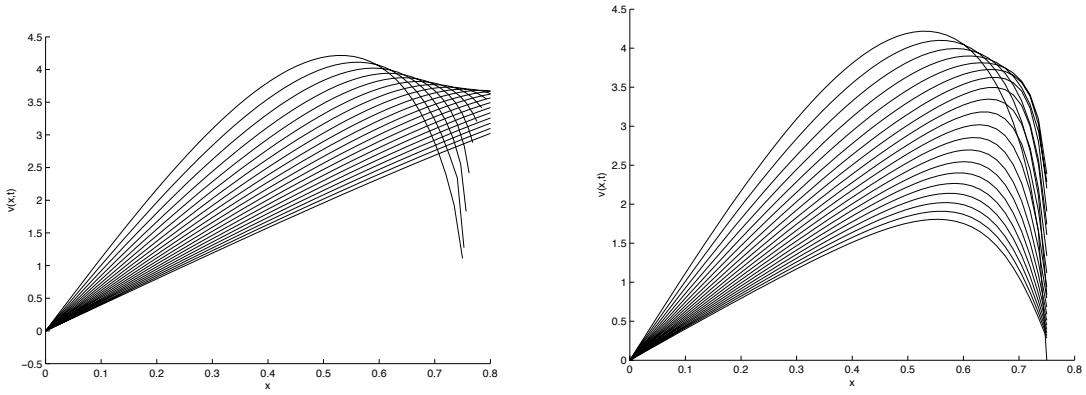

Figure 6.2: *Figure on the left shows the velocity that the moving mesh method calculates (see Chapter 7) and the figure on the right shows the numerical solution of equation (6.1).* $\alpha = 1.5$, $n = 1$.

time should occur. The numerical solution of the advection equation (6.1) shows that we should have a short waiting time and then a shock forms and the wave begins to move.

Using the same method for the TFE, we get an equation similar to (6.1), but due to it having many high order derivatives of v and u, the numerical solution of the equation would have been difficult to solve. A scheme such as the Adams/Bashforth 3rd order, 3 level scheme could have been implemented. We shall further discuss this in Chapter 10.

In the next chapter, we shall move on and derive the moving finite element method [3] for the PME and the TFE using the velocity (4.4) derived from the conservation of mass principle in chapter 4.

Chapter 7

Moving mesh explanation

In this chapter we shall construct the moving finite element method that will be used to numerically solve the PME and the TFE. It is an adaptive finite element method for solving PDEs with moving boundaries using a moving mesh. There are many advantages for using this method such as improved efficiency and for these particular problems, the lack of a need to locally remesh during computation.

Using the results from Chapter 4, if $u \neq 0$ it is possible to find the velocity of any interior mesh point in the domain using the equation

$$v = -u^{n-1}p_x$$

With the mesh velocities obtainable, we can now update the mesh position per time step by using a simple time-stepping method to solve $v = \frac{dx}{dt}$ for each node, and then the solution can be retrieved from equation (4.1). The mesh nodes will move so that within each interval, the conservation principle is satisfied.

Note that to find the velocity at the boundaries, we must take

$$v = -\lim_{u \to 0} u^{n-1}p_x$$

7.1 Finite Element Formulation

To solve this problem approximately using the finite element method, we introduce a test function into (4.1) and find the weak form of (4.2).

So, using the previous result, we propose a weak conservation principle with w being a test function advected with velocity v. w is continous and once differentiable.

$$\int_{x_{i-1}(t)}^{x_i(t)} w_i u dx = c \tag{7.1}$$

where c is a constant determined by the initial data. The partition of unity condition on w, is required for (7.1) to conserve mass

$$\sum_{j=0}^{N} w_j = 1$$

Differentiating (7.1) w.r.t. t leads to

$$\int_{x_{i-1}(t)}^{x_{i+1}(t)} w_i \frac{\partial}{\partial x} \left(u^n p_x + vu\right) dx = 0$$

assuming that w_i moves with v.

We assume that the test function will take the form of linear hat functions ϕ_i. These are defined as

$$\phi_j = \begin{cases} \frac{x - x_{j-1}}{x_j - x_{j-1}}, & x \in (x_{j-1}, x_j) \\ \frac{x_{j+1} - x}{x_{j+1} - x_j}, & x \in (x_j, x_{j+1}) \end{cases}$$

Integrating by parts and replacing w with ϕ_i, we get

$$\phi_i \left[u^n p_x + vu\right] \Big|_{x_{i-1}(t)}^{x_{i+1}(t)} - \int_{x_{i-1}(t)}^{x_{i+1}(t)} \frac{\partial \phi_i}{\partial x} \left[u^n p_x + vu\right] dx = 0$$

The term on the left vanishes since either $\phi_i = 0$ or $u = 0$ at the two boundaries, which results in

$$\int_{x_{i-1}(t)}^{x_{i+1}(t)} u \frac{\partial \phi_i}{\partial x} v dx = - \int_{x_{i-1}(t)}^{x_{i+1}(t)} u^n \frac{\partial \phi_i}{\partial x} \frac{\partial p}{\partial x} dx \tag{7.2}$$

The resulting matrix system on the left hand side of equation (7.2) is computationally difficult to solve as it is almost anti-symmetrical. To make this easier we shall define the velocity potential ψ given by

$$v = \frac{d\psi}{dx} \tag{7.3}$$

Substituting the finite element approximation of ψ

$$\psi = \sum_{j=0}^{N} \psi_j \phi_j \tag{7.4}$$

gives us a symmetric matrix on the left hand side of (7.2) resulting in a simpler system consisting of two weighted stiffness matrices

$$\int_{x_{i-1}(t)}^{x_{i+1}(t)} u \frac{\partial \phi_i}{\partial x} \frac{\partial \phi_j}{\partial x} \psi_j dx = - \int_{x_{i-1}(t)}^{x_{i+1}(t)} u^n \frac{\partial \phi_i}{\partial x} \frac{\partial p}{\partial x} dx$$

We shall now derive ψ individually for the PME and the TFE.

7.1.1 Getting ψ - Porous-Medium Equation

For the PME $p = u$ and we take the finite element approximation of u to be

$$u = \sum_{j=1}^{N} u_j \phi_j \tag{7.5}$$

We are now left with

$$\int_{x_{i-1}(t)}^{x_{i+1}(t)} u \frac{\partial \phi_i}{\partial x} \frac{\partial \phi_j}{\partial x} \psi_j dx = - \int_{x_{i-1}(t)}^{x_{i+1}(t)} u^n \frac{\partial \phi_i}{\partial x} \frac{\partial \phi_j}{\partial x} u_j$$

which leaves us with the symmetric matrix system to calculate the velocity potential ψ_j,

$$K(u)\underline{\psi} = -K(u^n)\underline{u}$$

Where K is a weighted tridiagonal matrix.

7.1.2 Getting ψ - Thin-Film Equation

As previously defined, u is piecewise linear. To approximate u_{xx}, we use a weak form of

$$p = -\frac{\partial^2 u}{\partial x^2} \tag{7.6}$$

Integrating equation (7.6) w.r.t. x, and taking the weak form,

$$\begin{aligned} \int_{x_{i-1}(t)}^{x_{i+1}(t)} \phi_i p dx &= - \int_{x_{i-1}(t)}^{x_{i+1}(t)} \phi_i \frac{\partial^2 u}{\partial x^2} dx \\ &= - \left[\phi_i \frac{\partial u}{\partial x} \right]_{x_{i-1}}^{x_{i+1}} + \int_{x_{i-1}(t)}^{x_{i+1}(t)} \frac{\partial \phi_i}{\partial x} \frac{\partial u}{\partial x} dx \end{aligned}$$

The first term on the right hand side vanishes as either $\phi_i = 0$ or due to the boundary conditions stated earlier. Taking the finite element approximation of u, defined in equation (7.5) and of p

$$p = \sum_{j=1}^{N} p_j \phi_j$$

we are left with

$$\int_{x_{i-1}(t)}^{x_{i+1}(t)} \phi_i \phi_j p_j dx = \int_{x_{i-1}(t)}^{x_{i+1}(t)} \frac{\partial \phi_i}{\partial x} \frac{\partial \phi_j}{\partial x} u_j dx$$

and we have the matrix system

$$M\underline{p} = K\underline{u}$$

This system will be solved for p, where M is the mass matrix and has the standard form.

We can now continue with method for the TFE in a similar fashion as with the PME, by first solving for p. Then we are left with the following system to solve for ψ

$$K(u)\underline{\psi} = -K(u^n)\underline{p}$$

As can be seen an extra system has to be solved when computing the numerical solution of the TFE. Once we have solved for ψ we follow the same method for both equations.

We integrate and take the weak form of (7.3) giving

$$\int_{x_{x-1}}^{x_{i+q}} \phi_i v dx = \int_{x_{x-1}}^{x_{i+q}} \phi_i \frac{d\psi}{dx} dx$$

Using the finite element approximation of ψ from (7.4) and taking the finite element approximation of v

$$v = \sum_{j=0}^{N} v_j \phi_j$$

we get the following equation to solve

$$\int_{x_{x-1}}^{x_{i+q}} \phi_i \phi_j v_j dx = \int_{x_{x-1}}^{x_{i+q}} \phi_i \frac{d\phi_j}{dx} \psi_j dx$$

This leaves us with the system

$$M\underline{v} = A\underline{\psi} \tag{7.7}$$

where A is defined as

$$A = \begin{pmatrix} 0 & -\frac{1}{2} & 0 & 0 & \dots & 0 \\ \frac{1}{2} & 0 & -\frac{1}{2} & 0 & \dots & \vdots \\ 0 & \frac{1}{2} & 0 & -\frac{1}{2} & 0 & \vdots \\ \vdots & \ddots & \ddots & \ddots & \ddots & \vdots \\ \vdots & \ddots & 0 & \frac{1}{2} & 0 & -\frac{1}{2} \\ 0 & \dots & \dots & 0 & \frac{1}{2} & 0 \end{pmatrix}$$

Now that we have v, we can update the mesh velocities using a time-step method. For the sake of ease, we shall use the explicit Euler scheme. This gives us

$$x_i = x_i + \Delta t v_i$$

The scheme unfortunately requires very small time-steps to ensure stability.

Finally, u must be solved on the new mesh. This is achieved by solving (7.1), where c is defined as follows

$$c = \int_{x_{i-1}(t_0)}^{x_{i+1}(t_0)} \phi_i u_0 dx$$

using the initial data u_0. Since c consists of the initial data only, it naturally remains the same for $t \geq 0$ This is due to it being defined as the total mass in the initial data, and this mass is kept constant by the conservation of mass principle.

So to get u back, we solve the system

$$M\underline{u} = \underline{c}$$

7.2 Implementing the method for computation

To solve these systems, the code was written in C++ for the PME, and for the TFE, FORTRAN was used due to its computational effiency and hence increase in speed. This was necessary as the time-steps for the TFE were approaching $10^{-10} - 10^{-12}$ and hence, a large number of iterations were required to study the behaviour of the numerical solution.

Due to oscillations and numerical instabilities, we had to use a number of adjustments to how the moving finite element method was implemented computationally. We shall look at these in turn.

7.2.1 Lumping of the mass matrix

Lumping is a method used primarily to reduce the computational expense of having to invert a matrix without a loss of accuracy.

In order to obtain a fully explicit scheme, the mass matrix is diagonalised or 'lumped'. Using the linear hat functions, lumping the matrix is achieved by adding all elements in each row of the mass matrix and placing the sum in the diagonal. Then, the lumped matrix replaces the mass matrix in the system. For more information on lumping, consult [22], [24] and for a more in depth discussion on the consequences of the use of lumping see [27].

7.2.2 Upwind method

When discretising a domain using piecewise linear elements, it is clear that the finite element method uses a similar 'stencil' as a central finite difference scheme.

This lead to the advection-diffusion behaviour of the velocity having numerical instabilities. An upwind finite element method was instead implemented. This lead to less oscillations, yet small localized oscillations were still occurring in the neighborhood of the steep gradient. For more information on this method see [10].

7.2.3 Smoothing method

Due to the small oscillations mentioned previously in the velocity of the numerical solution of the TFE, a smoothing method was used.

$$v_i = \frac{1}{4}v_{i-1} + \frac{1}{2}v_i + \frac{1}{4}v_{i+1}$$

This smoothing method eliminated some of the small oscillations that were occurring, and prevented blow up of the velocity. Unfortunately, due to the smoothing, the result was that we were computing a less accurate numerical solution. The smoothing of the moving front would have caused a lower velocity and hence a slightly longer waiting time, as was witnessed when comparing our results with Blowey et al [6].

Chapter 8

Numerical Results I

We now present numerical solutions using the methods described in Chapter 7. By also using the results in Chapter 5, we shall only examine results where a waiting time occurs. Bahattacharya [2] investigated the instant movement solutions without a waiting time using the same moving finite element method.

The solutions are plotted against the time dependent moving nodes, noting that the central node at $x = 0$ never moves due to it being the centre of mass. This is due to the symmetry of the initial conditions that we are solving both the TFE and the PME and the lack of any source term to either end of the domain (See Chapter 9 for an example of the effects of a source term).

8.1 Porous-Medium Equation Results

We shall begin by looking at the PME with two sets of values for α and n and comment on the observable features.

The results when using $\alpha = 4.5$ and $n = 1$ are shown in figures (8.1)

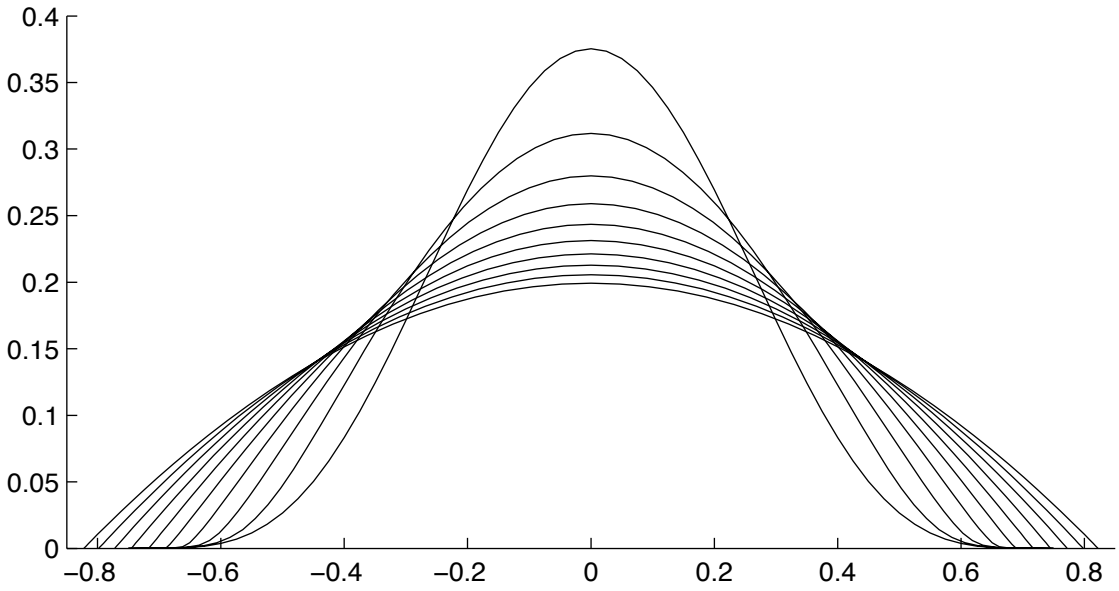

Figure 8.1: *Numerical solution of the PME with* $n = 1$, $\alpha = 4.5$

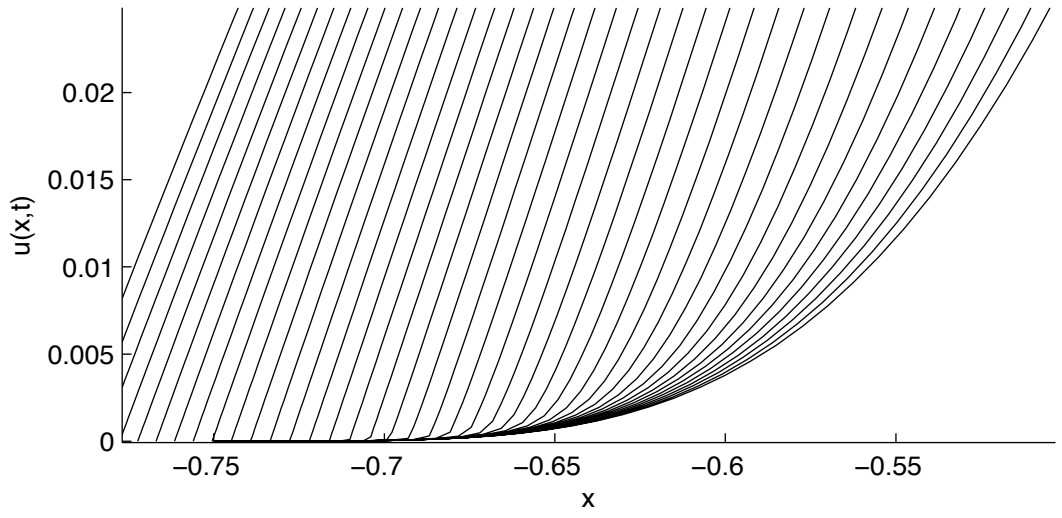

Figure 8.2: *Close up of the moving boundary of the numerical solution of the PME with* $n = 1$, $\alpha = 4.5$

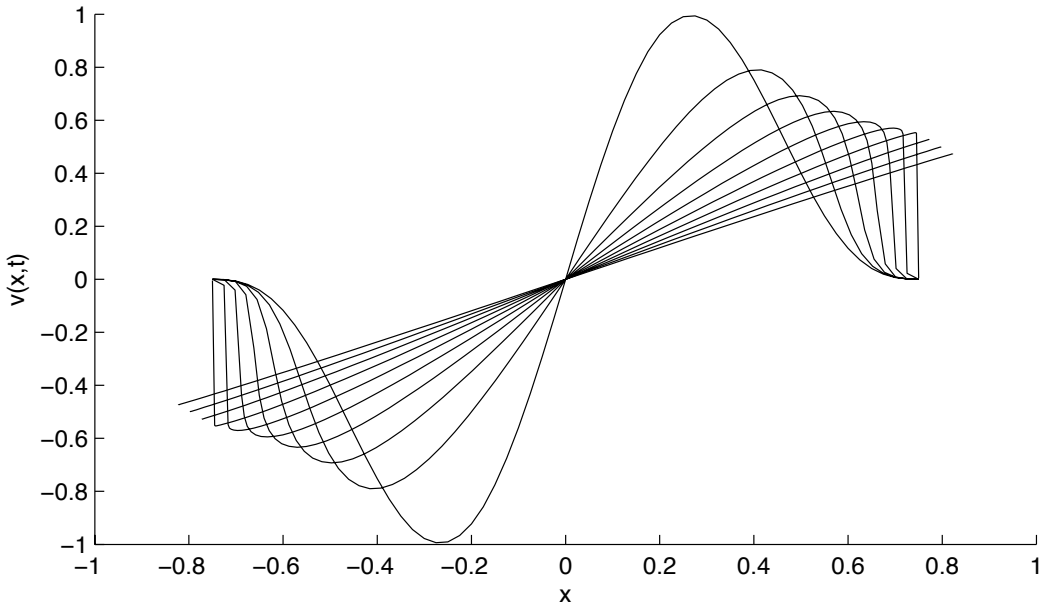

Figure 8.3: *Velocity's of the nodes of the numerical solution of the PME with* $n = 1$, $\alpha = 4.5$

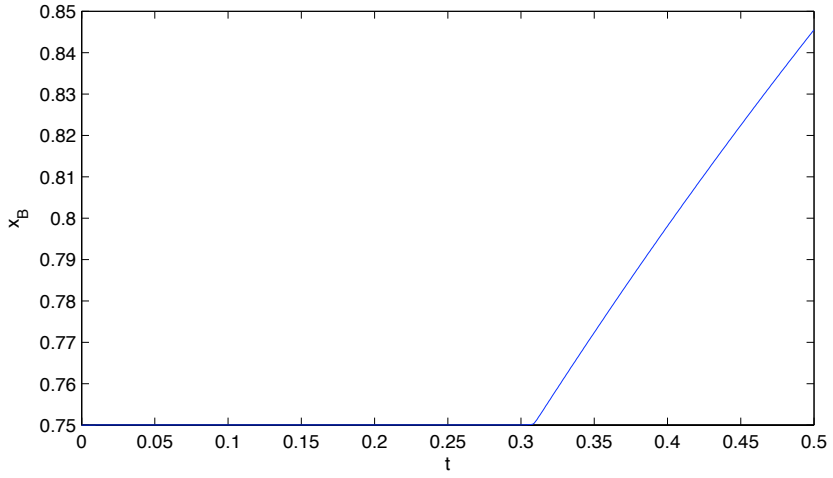

Figure 8.4: *Movement of the boundary of the PME with* $n = 1$, $\alpha = 4.5$

- (8.4). In figure (8.1) we see the expected waiting time occuring and also a clear profile redistribution behind the stationary boundary. This profile redistribution is more clearly seen in the close up of the boundary area in figure (8.2). The cover layer phenomenon observed in Kath and Cohens paper [12], can be clearly seen.

Figure (8.3) is really where our main interest lies and its the velocities advective profile that causes a shock to occur, and consequently, an immediate movement of the boundaries. In Chapter 6 we looked at solving an advection equation and concluded that, due to the limited fixed grid method used, it only gave information throughout the waiting time, but did not give any information on the movement of the boundaries after the waiting time. See Chapter 6 and the results in figure (6.1).

As can be seen, the velocities are positive when $x > 0$ and negative as $x < 0$. Over time a steepening front develops as t increases, which eventually becomes a shock. Also note that as in figure (6.1), the velocity is being diffused. After the shock we have a linear velocity that shall eventually tend to zero as $t \to +\infty$. Figure (8.4) shows the movement of the positive boundary and estimates a waiting time of duration $t = 0.31$.

Note that the moving finite element method coped very well with solving the PME, even when using the Euler method for the time-stepping. The time-steps to solve this without having an unstable solution were of order of magnitude 10^{-4} for 61 nodes.

We shall now look at another numerical solution with $\alpha = 0.5$ and $n = 7$. This again, using the results from Chapter 5, should give us a waiting time period due to the condition $n\alpha > 1$. With the value $\alpha = 0.5$, we get an entirely different profile for the intitial condition, compared with (8.1). This is an example of a non-zero contact angle, and due to the this, the waiting

time is a lot shorter because the required profile redistribution takes less time and hence the velocity forms a shock quicker.

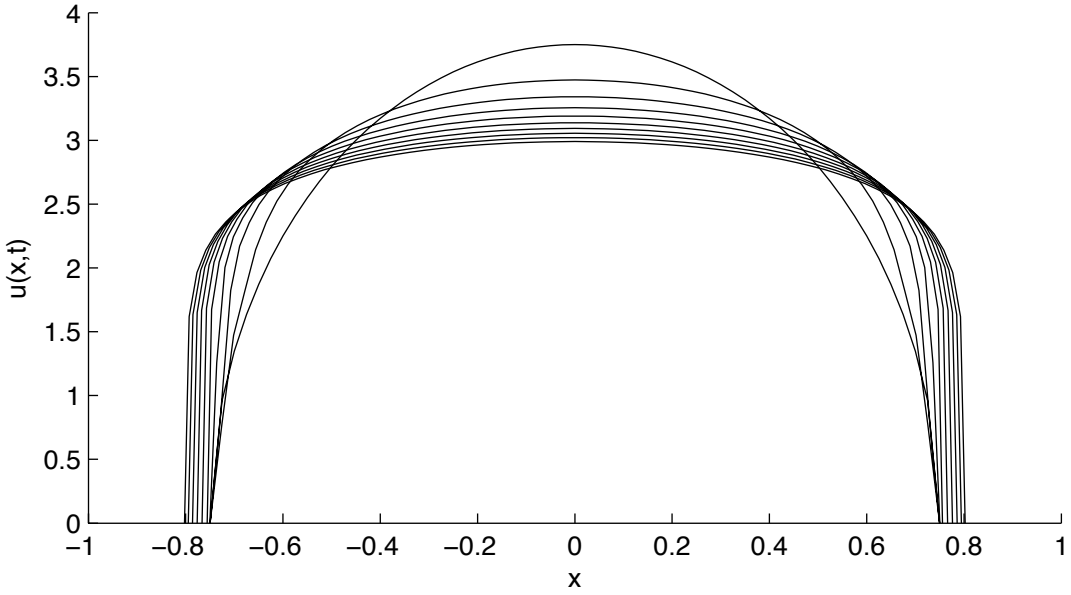

Figure 8.5: *numerical solution to the PME with* $n = 7$, $\alpha = 0.5$

Interestingly, in figure (8.6) due to the different contact angle, we do not see a corner layer present.

Figure (8.7) again shows a shock forming as the waiting time ends and the boundary begins to move. Due to setting $n = 7$, the diffusion is much stronger and this is most apparent in the velocity.

The waiting time is approximately $0.375 \times 10^{-}3$ as can be seen in figure (8.8), but is not as clearly defined as in the previous example.

8.2 Thin-Film Equation Results

We shall now concentrate on the numerical solutions of the TFE. It was expected that the velocity behaviour during the waiting time would be far more complicated and this can be seen occurring in figure (8.9). We observe

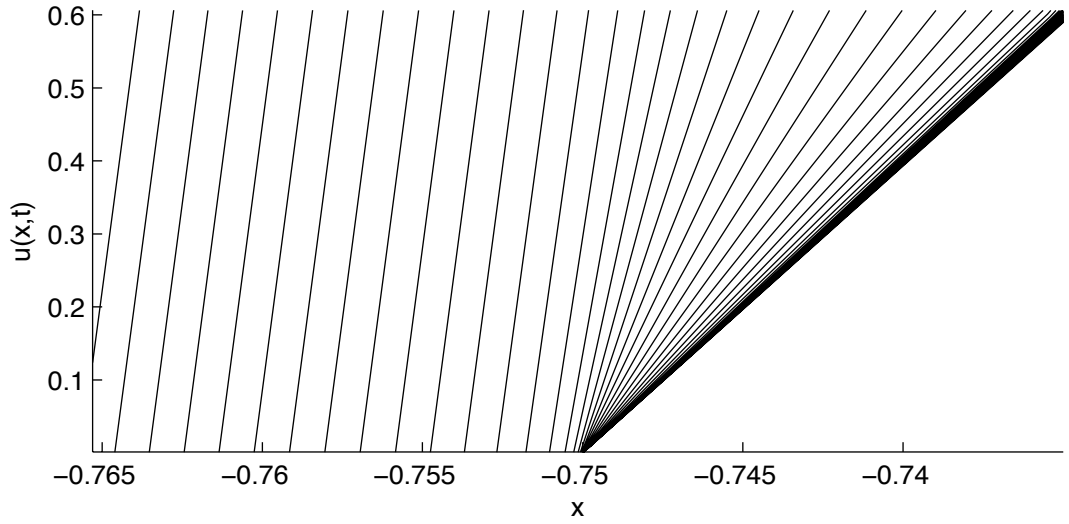

Figure 8.6: *Close up of the moving boundary of the numerical solution to the PME with* $n = 7$, $\alpha = 0.5$

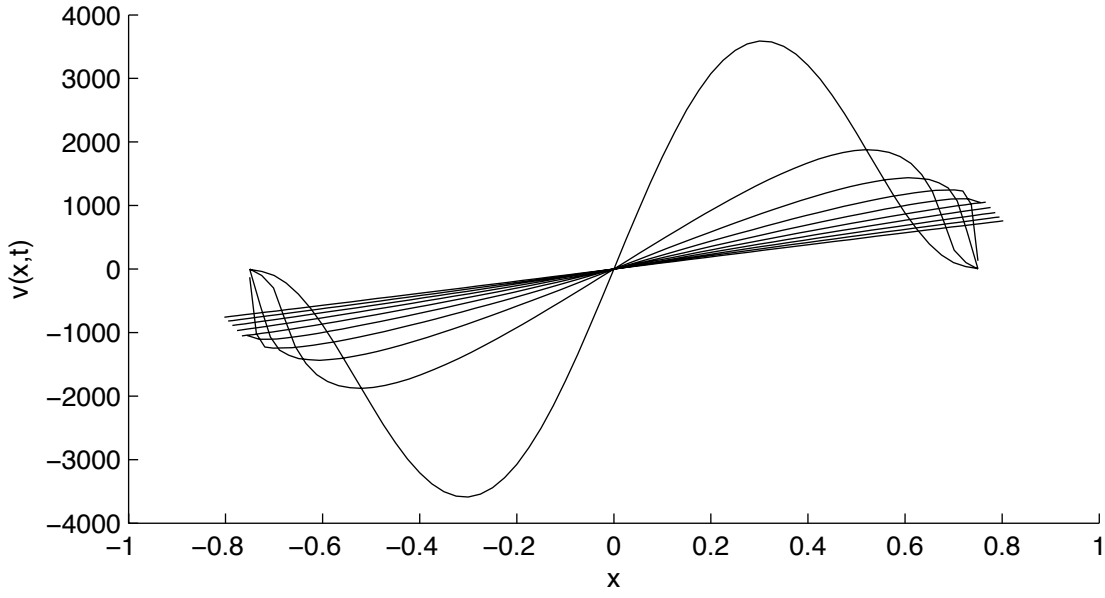

Figure 8.7: *Velocity of the nodes of the numerical solution to the PME with* $n = 7$, $\alpha = 0.5$

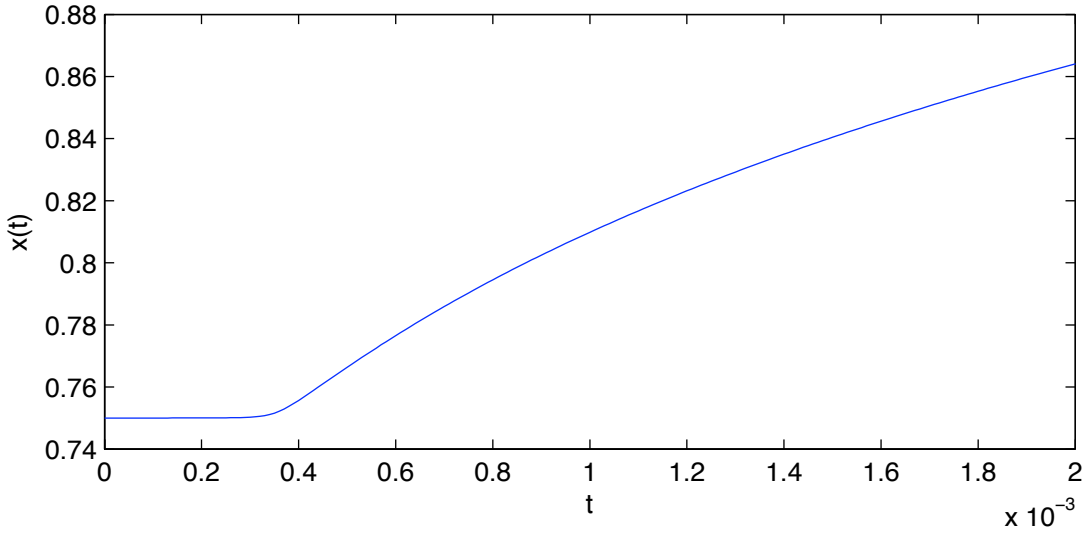

Figure 8.8: *Movement of the boundary of the PME with* $n = 7$, $\alpha = 0.5$

oscillations due to shocks forming within the domain rather than at the boundaries, as with the PME. As mentioned in Chapter 7, we used smoothing on v to supress the large oscillations, but by doing this we affected the shock formations and therefore the estimate for the waiting time was not as well approximated as for the PME.

Interestingly these oscillations in the velocity did not cause much disruption in u as can be seen in figure (8.9). Here we see similar results as with the PME, with a profile redistribution during the waiting time.

The velocity shows that certain nodes in the fluid move in the opposite direction. As can be seen in the high peaks, a shock forms within the domain, rather than at the boundary. We then get a movement akin to an advection equation, with the wave moving towards the boundary. The shock then reaches the boundary, and then as with the PME, we have a movement of the boundary.

Figure (8.11) shows the movement of the right hand boundary. Using these values of α and n gave us a chance to compare results with Blowey, King

and Langdons [6] results. The results gave a profile of u at a certain time-step. There was a slight difference in the results as the waiting time computed with the moving finite element method was slightly longer. This is most likely due to a smoothing of the shock, and hence the boundary in the solution we computed had not moved quite as far as what their numerical results showed This shall be discussed in more detail in Chapter 10, as there are changes to the methods used that could improve the results. Unfortunately due to time restrictions, these could not be implemented for this dissertation.

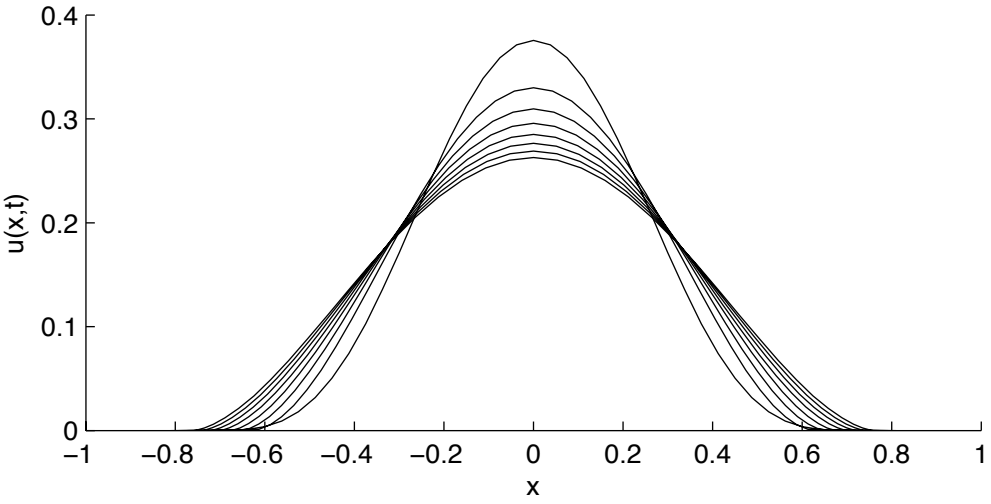

Figure 8.9: *Numerical solution of the TFE with* $n = 1$, $\alpha = 4.5$

We shall now very briefly comment on the final results which show more clearly what is occurring in the velocity during the waiting time.

As the shock begins to form it moves towards the boundary. It is diffused and clearly, the effects of the smoothing cause a few irregularities as it reaches the boundary. Figure (8.14) shows the waiting time as being approximately 0.285.

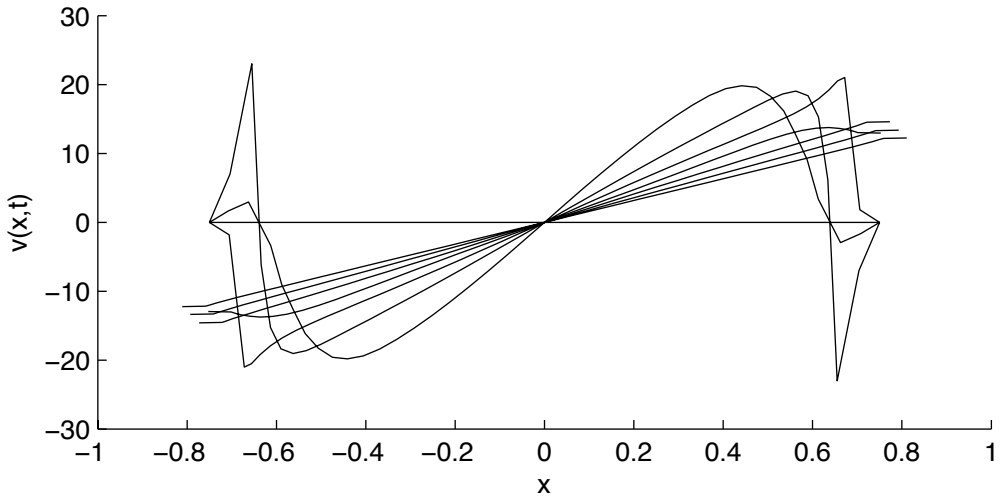

Figure 8.10: *Velocity of the nodes of the numerical solution to the TFE with* $n = 1$, $\alpha = 4.5$

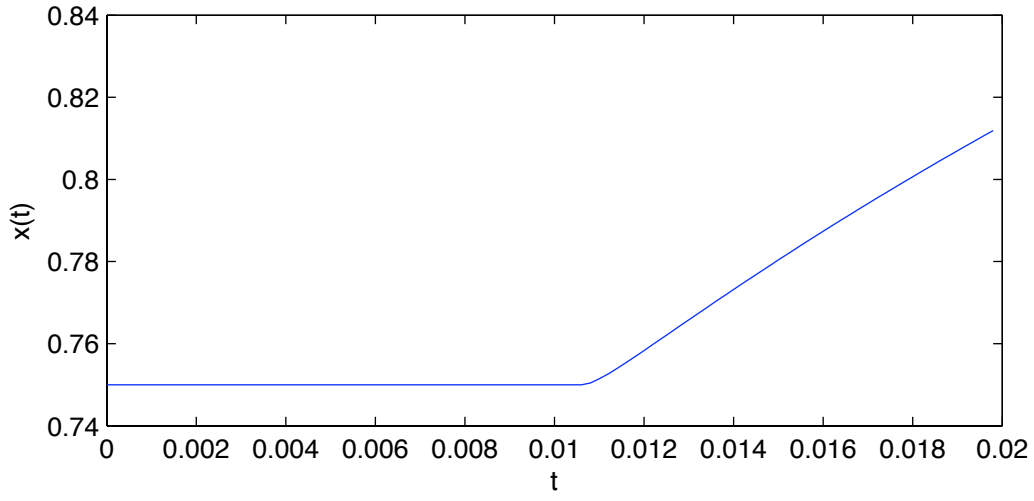

Figure 8.11: *Movement of the boundary of the TFE with plot* $n = 1$, $\alpha = 4.5$

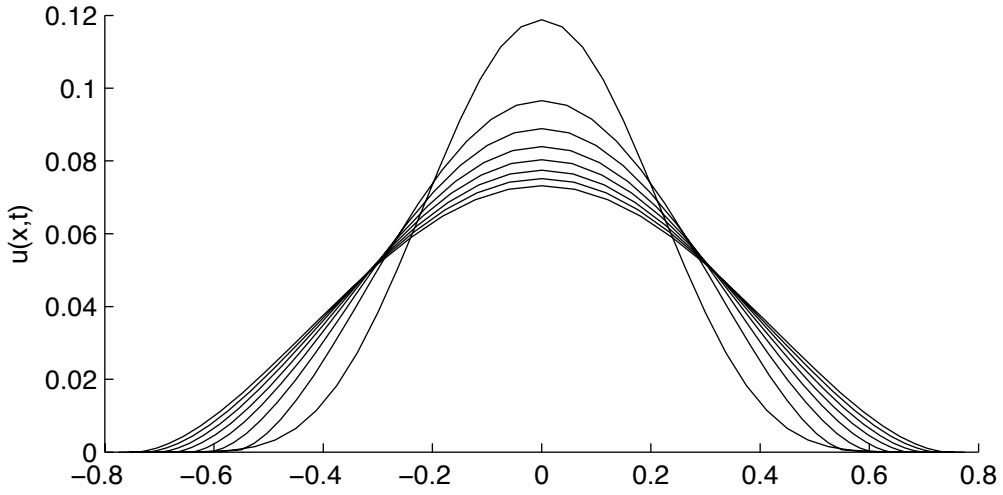

Figure 8.12: *Numerical solution to the TFE with plot* $n = 1$, $\alpha = 6.5$

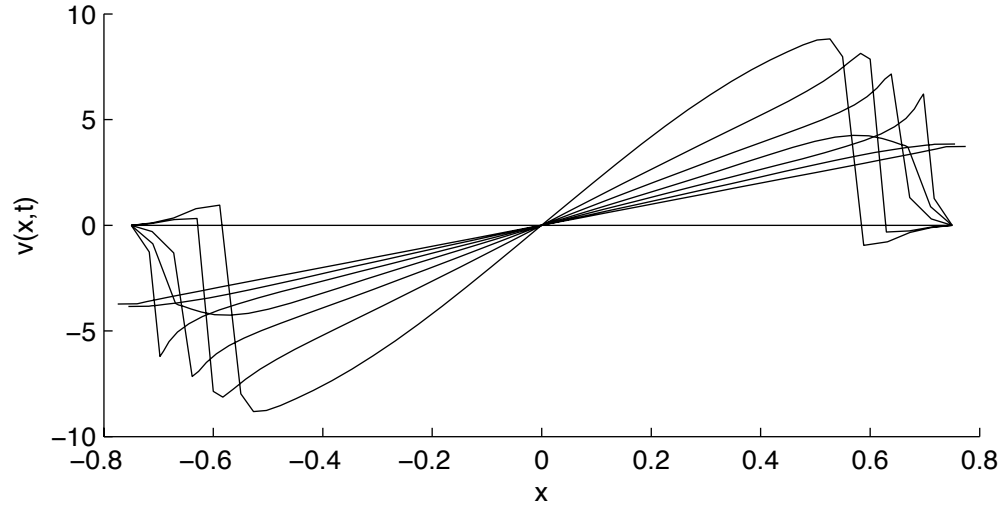

Figure 8.13: *Velocity of the nodes of the numerical solution to the TFE with plot* $n = 1$, $\alpha = 6.5$

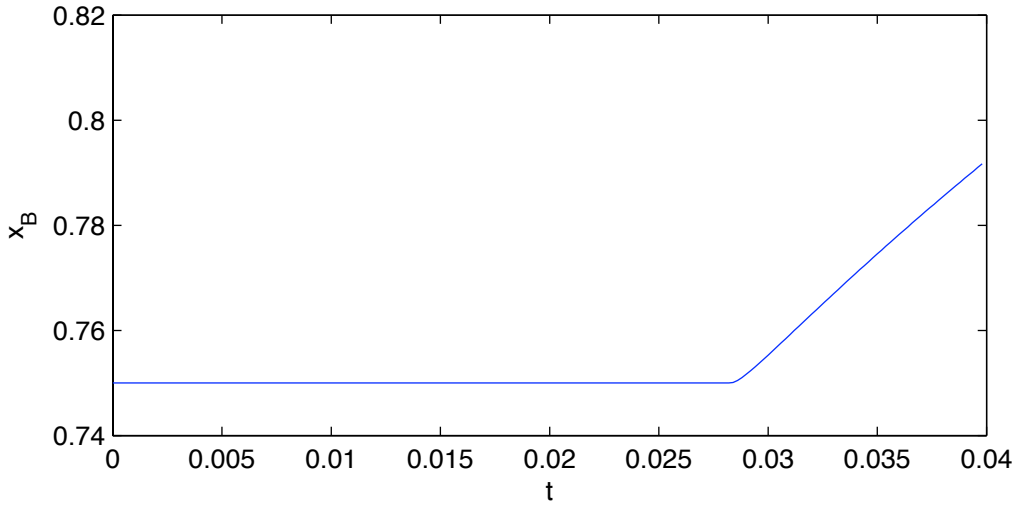

Figure 8.14: *Movement of the boundary of the TFE with plot* $n = 1$, $\alpha = 6.5$

In this chapter we have numerical solutions of both the PME and the TFE when the waiting time occurs. We have confirmed analytical results such as shock formation and waiting time occurrence and we have found that during the waiting time, the velocity acts similarly to the advection-diffusion equation that we numerically solved in Chapter 6. Importantly we also saw the movement of the boundary after the waiting time.

We shall now move on to the Richards' equation which models the flow of DNAPLs through soil, this requires a minor adjustment to the moving finite element method. Additionally, the analytical methods that we have used in this dissertation will be applied to this equation.

Chapter 9

Application: Richards' Equation

Non-linear diffusion was studied extensively by physicists modelling water flow in soils in the first half of the 20th century and one of the most important equations for soil moisture movement is the Richards' equation. It was based on work by Buckingham, and Gardner and Windtsoe [7] and deals with capillary pressure, but was left to Richards to formally express the nonlinear PDE to model this behaviour. It is derived from combining Darcy's law with the continuity equation to model unsaturated, non-steady state flow of water in the vertical direction.

The Richards' equation is a second order non linear diffusion equation and in that sense is similar to the PME.

$$s_t = [D(s)s_x + \kappa(s)\rho g]_z \tag{9.1}$$

where $s(z,t)$ is the saturation of the wetting phase, $\kappa(s)$ is the relative permeability to the wetting phase, and $D(s)$, the diffusion constant is of the form

$$D(s) = -\kappa(s)\frac{d\psi}{dz}(s)$$

where ψ us the capillary pressure. g is gravity which is acting downwards (negative z direction) and ρ is the density of the fluid being modelled. We assume that the specific water capacity of the soil is constant throughout the domain.

We shall take the same steps to non-dimensionalise equation (9.1), as in Grindrod's paper [9] and we arrive to the equation which shall be the basis of the remainder of this chapter. He assumed that $\psi(s) \propto s^{-1}$ and $\kappa(s) \propto s^k$, for some $k > 0$. Rescaling z and t we find

$$s_t = \left[D(s)s_z + \kappa(s)\right]_z \tag{9.2}$$

with $D(s) = s^{k-2}$ and $\kappa(s) = s^k$.

Setting $k = 2$, we have the Burgers equation. However, we shall concentrate on $k = 3$ as this is a good model for Creosote contamination in soil and there is an exact similarity solution involving Airey functions [9].

The aim of numerically solving this equation is to model the flow of DNAPLs in soil after infiltration. They can cause serious environmental problems and may contribute to groundwater contamination if they reach the water table.

The equation is very similar to the PME, and does not require a large change to the moving mesh method algorithm that was used in Chapter 7.

We shall examine the initial conditions as we did in Chapter 5 to obtain estimates of the values of the parameter α required for the waiting time phenomenon to occur.

But first, using the conservation of mass principle, we derive the velocity as in Chapter 4.

$$v = -\left(s_z + s^2\right) \tag{9.3}$$

and at the boundary the velocity is

$$v_B = -\lim_{s\to 0}\left(s_z + s^2\right) \tag{9.4}$$

9.1 Boundary behaviour at $t = 0$

Since the Richards' equation is of the same order as the PME, we expect the same general behaviour, a waiting time to exist for certain initial conditions.

The initial condition that shall be used is defined as follows

$$s(z,0) = \begin{cases} (1-z^2)^{\alpha} & \text{if } z \in [-1,1]; \\ 0 & \text{if } |z| > 1. \end{cases} \tag{9.5}$$

Analysing the initial conditions using the same method as in chapter 5, we substitute in (9.5) and its derivative into (9.4).

So,

$$v_B = -\lim_{s\to 0}\left(s_z + s^2\right) = \lim_{z\to z_B}\left(2\alpha z\left(1-z^2\right)^{\alpha-1} - \left(1-z^2\right)^{2\alpha}\right)$$

We shall look at both the left and right boundary, denoting v_B^+ be the boundary velocity for $z_B = 1$, and v_B^- be the boundary velocity for $z_B = -1$.

As can be seen we have three cases,

- if $\alpha > 1$, $v_B^+ = 0$, $v_B^- = 0$,
- if $\alpha = 1$, $v_B^+ = 2$, $v_B^- = -2$,
- if $0 < \alpha < 1$, $v_B^+ \to +\infty$ as $z_B \to 1$, $v_B^- \to -\infty$ as $z_B \to -1$.

See figure (9.1) and (9.2) for a plot of these results.

To observe the waiting time phenomenon using equation (9.5), we shall solve equation (9.2) for $\alpha > 1$. To solve this numerically we must slightly alter the method derived in Chapter 7.

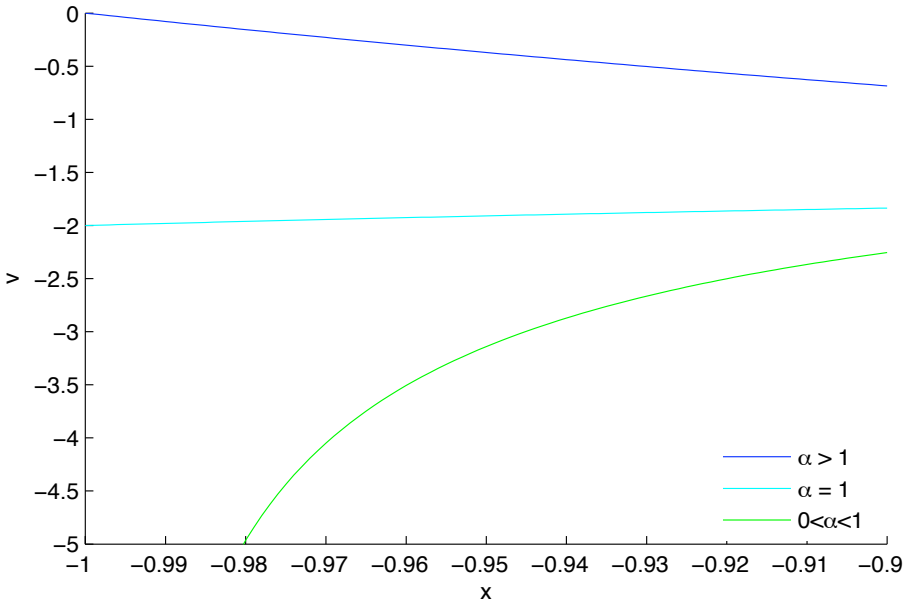

Figure 9.1: *Shows* v_B *as it tends to* $v_B^- = -1$

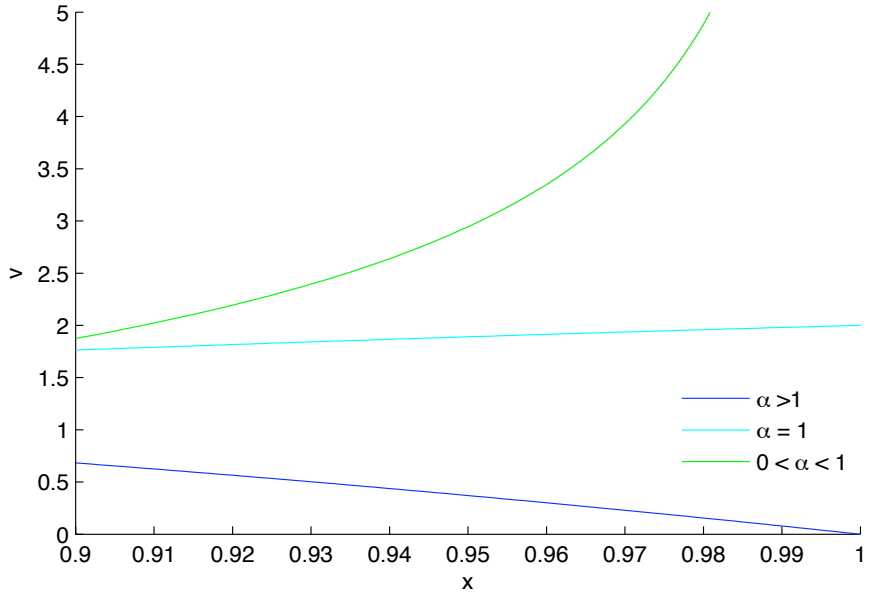

Figure 9.2: *Shows* v_B *as it tends to* $v_B^+ = -1$

9.2 Finite element formulation

We shall implement the same method as in chapter 7, but since equation (9.2) is different from the PME, as seen in the previous section, the velocity is also of a different form. These differences actually only alter the finite element method when finding ψ, so to avoid repetition, only this shall be separately derived.

We propose a weak conservation principle with w being a test function advected with velocity v and c is a constant determined by the initial conditions. w is continuous and once differentiable.

$$\int_{z_0}^{z_N} w_i s dz = c \tag{9.6}$$

where $c =$ constant. As previously, the partition of unity condition is required for equation (9.6) to conserve mass

$$\sum_{j=0}^{N} w_j = 1$$

Differentiating (9.6) w.r.t. t leads to

$$\int_{z_{i-1}(t)}^{z_{i+1}(t)} w_i \frac{\partial}{\partial z}\left(s s_z + s^3 + v s\right) dz = 0$$

We assume that the test function will take the form of linear hat functions ϕ_i as in Chapter 7.

So replacing w with ϕ_i and as before, we integrate by parts to get

$$\phi_i \left[s s_z + s^3 + v s\right]\Big|_{z_{i-1}(t)}^{z_{i+1}(t)} - \int_{z_{i-1}(t)}^{z_{i+1}(t)} \frac{\partial \phi_i}{\partial z}\left[s s_z + s^3\right] dz = 0$$

The first term on the left vanishes since either $\phi_i = 0$ or $s = 0$ at the two boundaries, so

$$\begin{aligned}\int_{z_{i-1}(t)}^{z_{i+1}(t)} s\frac{\partial \phi_i}{\partial z} v dz &= -\int_{z_{i-1}(t)}^{z_{i+1}(t)} \frac{\partial \phi_i}{\partial z}\left(s s_x + s^3\right) dz \\ &= \int_{z_{i-1}(t)}^{z_{i+1}(t)} s\frac{\partial \phi_i}{\partial z}\frac{\partial s}{\partial z} dz + \int_{z_{i-1}(t)}^{z_{i+1}(t)} \frac{\partial \phi_i}{\partial z} s^3 dz \qquad (9.7)\end{aligned}$$

Again we define the velocity potential and its finite element approximation and substitute this into (9.7)

$$\int_{z_{i-1}(t)}^{z_{i+1}(t)} s\frac{\partial \phi_i}{\partial z}\frac{\partial \phi_j}{\partial z}\psi_j dz = -\int_{z_{i-1}(t)}^{z_{i+1}(t)} s\frac{\partial \phi_i}{\partial z}\frac{\partial \phi_j}{\partial z} s_j dz + \int_{z_{i-1}(t)}^{z_{i+1}(t)} \frac{\partial \phi_i}{\partial z}\phi_j^3 s_j^3 dz \quad (9.8)$$

Now we have a symmetric matrix on the left hand side of (9.8) , resulting in the system

$$K(s)\underline{\psi} = -K(s)\underline{s} + B\underline{s}^3$$

where B is defined as

$$B = \begin{pmatrix} 0 & \frac{1}{4} & 0 & 0 & \dots & 0 \\ -\frac{1}{4} & 0 & \frac{1}{4} & 0 & \dots & \vdots \\ 0 & -\frac{1}{4} & 0 & \frac{1}{4} & 0 & \vdots \\ \vdots & \ddots & \ddots & \ddots & \ddots & \vdots \\ \vdots & \ddots & 0 & -\frac{1}{4} & 0 & \frac{1}{4} \\ 0 & \dots & \dots & 0 & -\frac{1}{4} & 0 \end{pmatrix}$$

Once we have ψ we continue as we did for the PME, solving for v and then updating the mesh positions. Finally we solve for s.

9.3 Numerical Results

The numerical results presented here are not compared to any known solutions. The solutions that Grindrod [9] constructed using Airey's functions, were not available and this will be commented on in Chapter 10. The program was known to be stable for the PME and was converging to known solutions without waiting times [2]. We conjecture that the solution will converge to some solution even though there are no known solutions of (9.2) that have the intitial conditions (9.5).

Initially when running the program, the velocity began to oscillate just before the shocks were forming at the boundaries. This was remedied using a smoothing function discussed in chapter 7. Minor oscillations are still apparent and this calls for further study of solving (9.2) using the moving mesh method. This shall be discussed more in the final chapter.

The additional s^3 term in (9.2) clearly affects the density distribution. Initially the density profile is symmetrical along the y-axis at $z = 0$, but after a few time-steps, the additional term moves the centre of mass to the left. This is not seen in the numerical solutions of the PME, where the solution stays symmetrical $\forall t$ and thus the centre of mass is always in the centre. Fig. (6.2)

This behaviour can also be observed in the velocity plot. The velocities are much higher in the domain to the left of the centre of gravity, compared with to the right. Also in the velocity plot, we can clearly see the two shocks forming just before the waiting time ends. The shocks form at different times to each other due to the differing velocities being applied to them. Clearly, the larger velocities at the left of the centre of mass are causing a shock to appear in a shorter time interval, hence a smaller waiting time compared with the boundary at $z = 1$.

As an example of an application of this numerical solution, we shall define

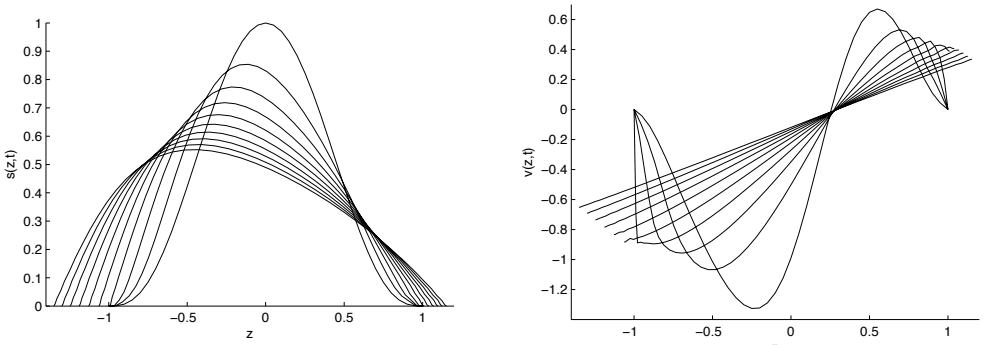

Figure 9.3: *Numerical solution of s and the corresponding mesh velocites v showing two seperate shocks forming at different times,* $\alpha = 3.0$

the water table at $z = -3$. The solution can predict the time at which the moving liquid (DNAPL) reaches the water table and interacts with the water, therby contaminating it.

Figure (9.4) shows the solution for $\alpha = 3.0$ up until the boundary reaches $z = -3$. It reaches this value at $t = 6.55$. Physically, the contact angle of the initial data is influenced by α, and hence a lower value would cause the fluid to reach the water table at a quicker rate. Hence, as shown for the PME, the initial profile of s affects the waiting time.

This investigation has been limited to certain values of n and α and does not use initial conditions derived from analytical solutions. It is hence limited in this sense but the application is interesting enough alone for the further study of this problem.

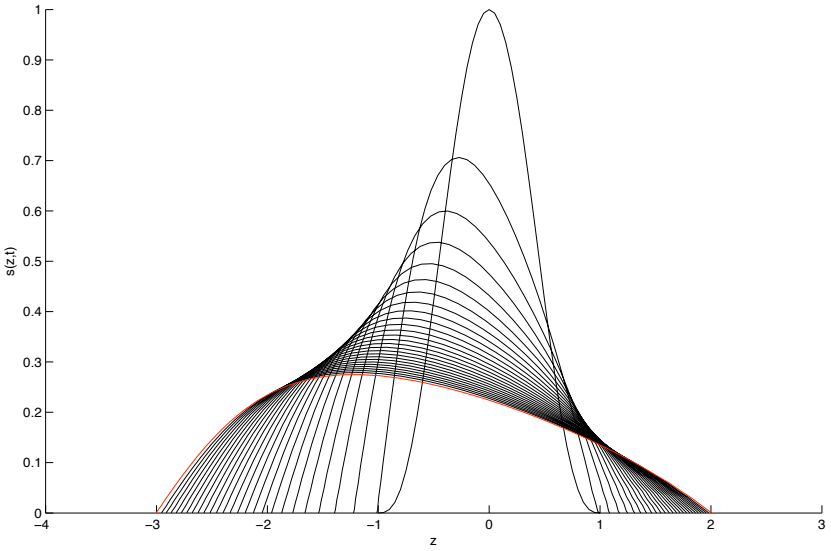

Figure 9.4: *Numerical solution of s as it approaches the water table set at $z = -3$ $\alpha = 3.0$*

Chapter 10

Conclusions and Further Work

10.1 Summary

This dissertation has illustrated the various techniques for finding out properties of the waiting time of the solutions of parabolic PDES, specifically the PME and the TFE. The motivation for studying the waiting times began with B. Bhatachyras dissertation [2] where she briefly commented on waiting times after implementing a moving mesh method on the 4th and 6th order non-linear diffusion equations based on a conservation of mass principle, and also the subsequent derivation of the advection-diffusion equation for the velocity. This final chapter serves as a summary of the work presented and suggests possible future avenues of study.

We began by defining the PME, TFE and the Richards' equation and explains the possible applications to each as a motivation for further study. We continue with a brief description of the literature that is available for them and mention some key analytical and numerical results. In Chapter 3 we begin to focus on the main topic of the dissertation. We examine the literature currently available on the waiting time phenomenon, looking again at the analytical and numerical results presented and also mention a

few physical processes that these equations can be applied to. We derive a velocity which satisfies the conservation principle within each interval in the domain in Chapter 4. This derivation is fundamental for the remainder of the dissertation. In Chapter 5 we do an analysis on specific initial data for both the 2nd and 4th order equations, and find the conditions that predict that a waiting time will occur based on the initial velocity at the boundary. We then derive an advection-diffusion equation for v using the velocity equation from Chapter 4. Using the method of characteristics we show that a shock will appear, and then we numerically solve this equation using a fixed grid finite difference method. We find that this numerical solution is only useful during the waiting time and therefore it doesn't give us any information on what happens to the numerical solution once the boundary begins to move.

In Chapter 7 we use the conservation principle from Chapter 4 and we derive a moving mesh method and construct a finite element formulation for its solutions. Chapter 8 presented the numerical results from the previous chapter and we explained what was happening for each separate solution. We found that we had very similar behaviour to the advection-diffusion velocity equation and once the boundary began to move, the velocity became nearly linear across the domain and tended to zero as $t \to +\infty$, $\forall x$. In Chapter 9 we extended the analytical and numerical methods to the Richards' equation and found that the numerical solution, as expected, was non-symetrical, and this gave us a separate waiting time for each boundary. In general though, we observed similar behaviour compared with the PME.

10.2 Further Work

In this section we shall look at some of the possible extensions to what was investigated in this dissertation and also consider how certains parts could

be improved on.

10.2.1 Advection-Diffusion velocity equation for the TFE

As mentioned in Chapter 6, the advection-diffusion equation derived for the velocity had high order derivatives which would have been difficult to solve numerically. This was therefore not looked at due to time constrictions. If a numerical solution were to be obtained, an approximation to the waiting time could be found and we may also see more clearly what happens to the velocity just before the final shock forms at the boundary.

10.2.2 Improving the stability of the TFE finite element method

At the end of Chapter 7 we briefly discussed the use of an upwind finite element method. We were still able to see the shocks forming, and the movement towards the boundary, but the oscillations were not giving us as clear a picture as was wanted. This needs to be investigated further due to the possibility of computing a more stable numerical solution and an improvement to the approximation of the waiting time.

10.2.3 Richards' Equation

Richards' equation was only touched upon in chapter 9 for the case $k = 3$. It gave a new insight into the waiting time phenomenon as the two boundaries had differing behaviour due to the weighting factor of the extra term in the Richards equation, compared with the PME, causing it to be non-symmetrical in the line $x = 0$.

We also encountered localised oscillations near the boundary as the shock formed, and again as for the TFE, we used the smoothing method to supress these to give a clearer understanding of what was occuring. The smoothing does affect the overall solution though, and with some adjustment to the computational adaptation of the moving finite element method, the smoothing could be eliminated, thus giving a more accurate waiting time.

The use of initial conditions that have been derived from exact analytical solutions would give a chance to compare the numerical solution to the exact solution to see the accuracy of the method and wether it converges to the exact solution or not.

The equation is used in soil science and would benefit further study due to its important environmental applications in the flow of pollutants in contaminated soils.

Bibliography

[1] D. G. Aronson. Regularity properties of flows through porous media: A counter-example. *J. Appl. Math.* **19** (1970)

[2] A moving mesh finite element method for high order non-linear diffusion problems with moving boundaries. *Unpublished*

[3] M. J. Baines, M. E. hubbard, P. K. Jimack. A moving mesh finite element algorithm for the adaptive solution of time-dependent partial differential equations with moving boundaries. *App. Num. Maths.* **54** (2005)

[4] G. I. Barenblatt, E. Beretta, M. Bertsch. The problem of a spreading of a liquid film along a solid surface: A new mathematical formulation. *Proc. NatU. Acad. Sci. USA* **94** (1997)

[5] K. W. Blake. Moving Mesh Methods for Non-Linear Parabolic Partial Differential Equations. *PhD Thesis* (2001)

[6] J. F. Blowey, J. R. King, S. Langdon Small and waiting-time behaviour of the thin-film equation *to appear in .....*

[7] Gardner, W., and J.A. Widtsoe. The movement of soil moisture. *Soil Sci.* **11** (1921)

[8] J. Gratton, C. Vigo. Evolution of self-similarity, and other properties of waiting-time solutions of the porous medium equation: the case of viscous gravity currents. *Euro. Jnl of Applied Math.* **9** (1998)

[9] P. Grindrod. Ricatti Rides Again. *Private communication*

[10] A.N. Brooks T.J.R Hughes. Streamline upwind/Petrov-Galerkin formulations for convection dominated flows with particular emphasis on the incompressible Navier-Stokes equations. *Comput. Method Appl. Mech. Engrg.* **32** (1982)

[11] Jie Li, Marc Hesse, Johanna Ziegler, Andrew W. Woods. An arbitrary Lagrangian Eulerian method for moving-boundary problems and its application to jumping over water. *J. Comp. Phy.* **208** (2005)

[12] William L. Kath, Donald S. Cohen. Waiting-Time Behaviour in a Nonlinear Diffusion Equation. *SIAM* **67** (1982)

[13] B. F. Knerr. The porous medium equation in one dimension. *Amer. Math. Soc.* **234** (1977)

[14] P. Y. Polubarinova-Kochina. Theory of Ground Water Movement. *Princeton U.P.* 1962

[15] A. A. Lacey, J. R. Ockendon and A. B. Tayler. "Waiting-time solutions of a nonlinear diffusion equation. *SIAM J. of Appl. Maths.* **42** (1982)

[16] S. Langdon Thin film equation, small-time conjectures and numerical results. *Private Communications*

[17] E. Momoniat, D. P. Mason, F.M Mahomed. Non-linear diffusion of an axisymmetric thin liquid drop: group-invariant solution and conservation law. *Int Journal of Non-Linear Mechanics* **36** (2001)

[18] E. Momoniat, D. P. Mason. Spreading of a thin film with suction or blowing including surface tension effects. *Comp. and Math. with Applications.* **53** (2007)

[19] M. Muskat, The flow of homogeneous fluids through porous media. *McGraw-Hill* 1937

[20] T. G. Myers Thin films with high surface tension. *SIAM Rev.* **40** (1998)

[21] O. A. Oleinik, A. S. Kalashnikov, S. Yui-Lin. The Cauchy problem and boundary problems for equations of the type of unsteady filtration. *Izv. Akad. Nauk SSSR Ser. Mat.* **22** (1958)

[22] D. W. Pepper, J. C. Heinrich. The Finite Element Method: Basic Concepts and Applications. *Taylor and Francis*

[23] J.R. Philip. Exact solutions for redistribution by nonlinear convertion-diffusion. *J. Austral. Math. Soc. Ser.* **33** (1992)

[24] L. J. Segerlind. Applied Finite Element Analysis. *Wiley* 1984

[25] N. F. Smyth and J. M. Hill. High order Nonlinear Diffusion. *IMA J. of App. Math.* **40** (1988)

[26] P.Wesseling. Computational fluid dynamics. *Springer* 2000

[27] O. C. Zienkiewicz. Finite Element Method for Solid and Structural Mechanics. *McGraw-Hill* 1971